Acta Crystallographica Section B
Structural Science
ISSN 0108-7681

Quininium (*R*)-mandelate, a structure with large *Z*′ described as an incommensurately modulated structure in (3+1)-dimensional superspace

Andreas Schönleber[a]*‡ and Gervais Chapuis[b]

[a]Institut de Cristallographie, Université de Lausanne, BSP-Dorigny, CH-1015 Lausanne, Switzerland, and [b]Laboratoire de Cristallographie–IPMC–FSB, École Polytechnique Fédéral de Lausanne, BSP-Dorigny, CH-1015 Lausanne, Switzerland

‡ Present address: Dpto de Física de la Materia Condensada, Facultad de Ciencia y Tecnología, Universidad del País Basco, Apdo 644, 48080 Bilbao, Spain.

Correspondence e-mail: wmxscxxa@lg.ehu.es

Received 14 October 2003
Accepted 1 December 2003

Quininium (*R*)-mandelate, $C_{20}H_{25}N_2O_2^+\cdot C_8H_7O_3^-$, is an organic salt with an incommensurately modulated structure. The superspace approach is required for a precise description of the structure at room temperature. In addition to the main reflections, the diffraction pattern also exhibits higher-order satellite reflections. The large number of first- and second-order satellite reflections with relatively strong intensities indicates a significant modulation. No average structure solution could be obtained on the basis of the main reflections only and hence the structure solution was performed in two suitable superstructure approximations, including satellite intensities. Positional modulation functions and modulation functions for the anisotropic atomic displacement parameters were introduced. The modulation originates from a competition between intramolecular and intermolecular forces, which is reflected, in the superspace formalism, in the modification of hydrogen bonds along the internal space variable *t*.

1. Introduction

Quinine, $C_{20}H_{24}N_2O_2$, is a 6′-methoxy (8α,9*R*)-cinchonan-9-ol (Lide & Frederikse, 1995). Owing to its long-time use as an antimalarial, antibacterial and cardio-active agent, the chemistry and biological activity, molecular structure, and preferred conformations of quinine have been widely studied. Along with quinidine, cinchonidine and cinchonine, quinine is a member of the *cinchona* group. These four alkaloids have the chiral C atoms C03, C04, C08 and C09 [the atom labelling is adopted from Oleksyn (1980) and is presented in Fig. 1], with the same absolute configuration at atoms C03 and C04 (3*R*,4*S*) but the opposite configuration at atoms C08 and C09 (Oleksyn, 1980). The substituent at atom C19 can be also changed (Table 1). Nevertheless, in the crystalline state, the molecular structures of all four *cinchona* alkaloids are similar. In salts, they are protonated and form cations. Most often, the protonated quinuclidinium atom N01 (N01 acts as a hydrogen-bond donor) interacts with the anion *via* N01—H01$\cdots$*A* [with *A* being the acceptor] hydrogen bonds (Dupont *et al.*, 1985; Oleksyn & Serda, 1993).

The overall molecular shape of the quininium cation can be characterized by the relative position of two main moieties, *viz.* the bicyclic planar quinoline and the bicyclic quinuclidine, in which all the rings are in a boat conformation. The conformation is expressed by characteristic torsion angles. The similarities of the torsion angles for various crystalline environments indicate a high stability for a specific conformation. As a consequence, the overall shapes of the molecules are similar. A rigid-body-motion analysis of cinchonine has shown, however, that it is not possible to regard the whole

molecule as rigid because of the strong internal libration of the quinuclidine group around the C08—C09 bond and independent vibrations of the vinyl C10/C11 group (Oleksyn *et al.*, 1979).

Mandelic acid, $C_8H_8O_3$, is an α-hydroxy benzeneacetic acid (Lide & Frederikse, 1995). The molecule itself has one chiral C atom (C28; for the atom labelling see Fig. 1; the carboxy O atom with the smaller O—C25—C28—O29 torsion angle is defined as atom O26 and the phenyl C atom that is positioned *anti* to atom O29 is defined as atom C31. The mandelic acid molecule can be defined by two groups, namely the planar phenyl ring and the carboxylate group. This molecule exhibits an almost planar arrangement of the carboxy and hydroxy groups as a preferred conformation in the mandelate anion (Larsen & Lopez de Diego, 1993), and hence the overall conformation of the mandelate anion is well described by the torsion angles between these two units.

The following non-modulated salt structures of *cinchona* alkaloids with mandelic acid have already been published: cinchoninium (*S*)- and (*R*)-mandelate (Larsen *et al.*, 1993), cinchonidinium (*S*)- and (*R*)-mandelate (Gjerløv & Larsen, 1997*a*), and quininium (*S*)-mandelate (Gjerløv & Larsen, 1997*b*). All of these compounds crystallize as classical three-dimensional periodic structures, despite the static disorder observed in the vinyl group (C10/C11) in cinchoninium (*R*)-mandelate. Only the structure of quininium (*R*)-mandelate shows a modulation and it has been suggested that this structure is commensurately modulated (Gjerløv *et al.*, 1995).

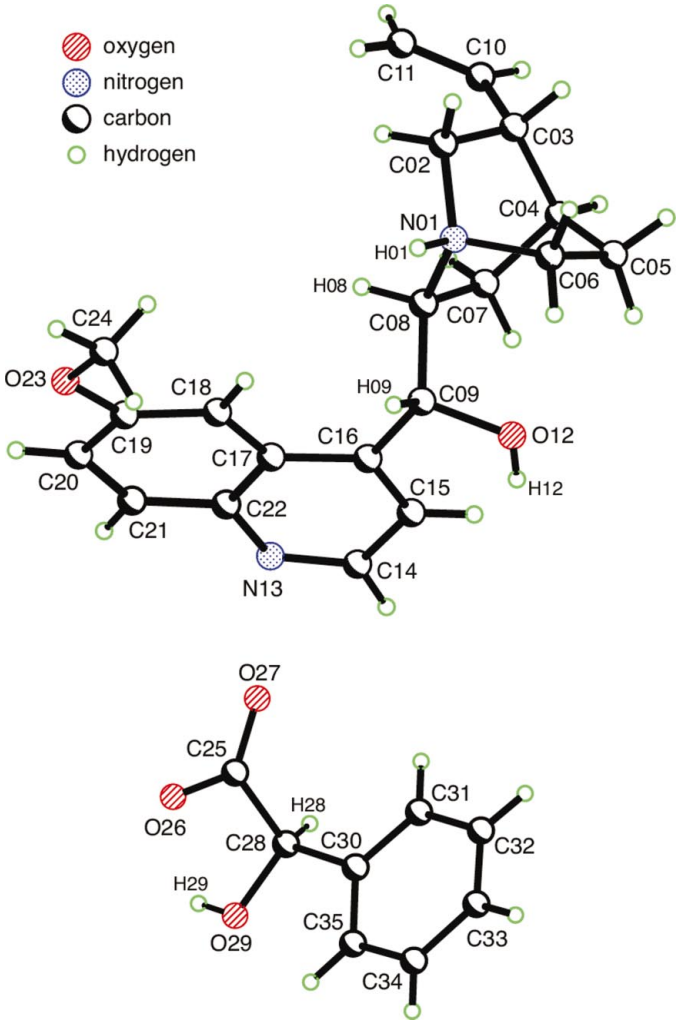

Figure 1
The molecular structure and atom labelling (adopted from Oleksyn, 1980) of the quininium cation (top) and the mandelate anion (bottom).

Table 1
The different substituents of cinchona alkaloids at C19 and their absolute configurations in C08 and C09 (Oleksyn, 1980).

		Configuration in	
	Substituent at C19	C08	C09
Quinine	$-OCH_3$	*S*	*R*
Quinidine	$-OCH_3$	*R*	*S*
Cinchonidine	–H	*S*	*R*
Cinchonine	–H	*R*	*S*

The aim of the present article is to present a new model and to interpret and describe the structure of quininium (*R*)-mandelate as an incommensurately modulated structure by applying the (3+1)-dimensional superspace approach (de Wolff, 1974; van Aalst *et al.*, 1976; Janssen & Janner, 1987; Janssen, 1988; van Smaalen, 1995; Yamamoto, 1996). A single-crystal X-ray diffraction experiment was performed at room temperature. The structure was solved in three-dimensional space in two superstructure approximations, with $Z' = 15$ and $Z' = 18$. [Z' is the number of independent molecules per asymmetric unit or, more strictly, the number of formula units in the unit cell divided by the number of independent general positions (Brock, 1996; Steed, 2003).] The origin of the modulation might be found in competition between the preferred conformations of the molecules and the hydrogen-bond motif, *i.e.* between intramolecular and intermolecular forces.

2. Experimental

2.1. Sample preparation

Crystals were obtained by dissolving quinine (0.76 g, 0.005 mol), $C_{20}H_{24}N_2O_2$ (purum DAB; ≃99%; Fluka), and (*R*)-mandelic acid (1.62 g, 0.005 mol), $C_8H_8O_3$ (puriss.; > 99%; Fluka), each in methanol (30 ml), CH_3OH (for analysis; > 99.8%; Merck). All compounds were used as purchased without further purification. A solution of the acid was neutralized with a solution of the base and the mixture was stirred for a few minutes. After complete evaporation of the solvent, the remaining microcrystalline white powder was dissolved in warmed methanol (100 ml; to guarantee complete dissolution of the residue) for slow recrystallization, giving single crystals suitable for the diffraction experiment. The colourless, transparent and needle-shaped crystals are stable in air; no further protection was necessary.

Table 2
Overview of the three measurements M1, M2 and M3.

	M1	M2	M3
Exposure time (min)	15	7	3
No. of reflections (all, main, satellites)	77078, 6280, 70798	62899, 6135, 56764	64377, 8242, 56135
No. of refused overlapped reflections	76221	62944	33086
No. of overflows	97	35	1
Criterion for observed reflections	$I \geq 2\sigma(I)$	$I \geq 2\sigma(I)$	$I \geq 2\sigma(I)$
$\langle I/\sigma(I)\rangle$ for observed main and satellite reflections (order 1, 2, 3, 4, 5)	32.10, 20.04, 8.72, 4.38, 3.10, 2.58	28.19, 15.39, 6.56, 3.68, 2.78, –	20.49, 10.08, 4.75, 3.05, –, –
Range of h, k, l, m	$-8 \Rightarrow h \Rightarrow 8$ $-21 \Rightarrow k \Rightarrow 21$ $-13 \Rightarrow l \Rightarrow 13$ $-5 \Rightarrow m \Rightarrow 5$	$-8 \Rightarrow h \Rightarrow 8$ $-21 \Rightarrow k \Rightarrow 21$ $-13 \Rightarrow l \Rightarrow 13$ $-4 \Rightarrow m \Rightarrow 4$	$-8 \Rightarrow h \Rightarrow 8$ $-21 \Rightarrow k \Rightarrow 21$ $-12 \Rightarrow l \Rightarrow 12$ $-3 \Rightarrow m \Rightarrow 3$
Scale [on basis $I > 10\sigma(I)$]	1.000	2.286 (2)	3.921(5)

Computer programs used: *X-AREA* (Stoe & Cie, 2002), *JANA*2000 (Petricek & Dusek, 2003).

2.2. Data collection

The quality of the crystals was tested with an optical binocular under polarized light and by X-ray diffraction precession photographs (Fig. 2). The crystals were not twinned but single domains. The extinction obliquity with respect to the edge parallel to the longest dimension of the crystal is about $\varphi \simeq 40°$.

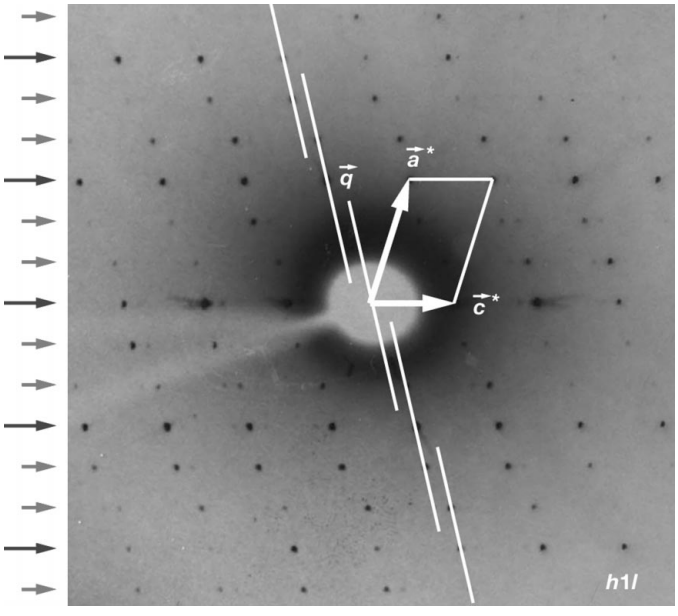

Figure 2
The centre of a precession photograph (Cu $K\alpha$) of the $h1l$ layer at room temperature. The unit cell ($\mathbf{a}^*, \mathbf{c}^*$) and the modulation vector ($\mathbf{q} = 0.333\mathbf{a}^* - 0.271\mathbf{c}^*$) are indicated. The long arrows on the left-hand side indicate lines of main and third-order satellite reflections; the short arrows indicate those of first- and second-order satellite reflections.

Table 3
Experimental data.

Crystal data	
Chemical formula	$C_{20}H_{25}N_2O_2^+ \cdot C_8H_7O_3^-$
Chemical formula weight	476.57
Temperature (K)	291 (1)
Crystal system, superspace group	Monoclinic, $P2_1(\alpha 0 \gamma)$
a, b, c (Å)	6.614 (3), 18.552 (7), 10.377 (4)
β (°)	107.47 (3)
Modulation wavevector	0.3329 (2), 0, −0.2713 (4)
V (Å^3)	1214.6 (9)
Z	2
D_x (Mg m^{-3})	1.3027 (9)
$F(000)$	508
Crystal form, colour	Platelet, colourless, transparent
Crystal size (mm)	0.24 × 0.18 × 0.08
No. of reflections for cell parameters	7295
2θ range (°)	4.04–49.17
Data collection	
Diffractometer	Stoe IPDS II
Radiation type	Mo $K\alpha$
Absorption correction	None
μ (mm^{-1})	0.090
Data collection method	ω scan
Range of h, k, l, m	$-8 \Rightarrow h \Rightarrow 8$ $-21 \Rightarrow k \Rightarrow 21$ $0 \Rightarrow l \Rightarrow 13$ $-5 \Rightarrow m \Rightarrow 5$
No. of measured, independent and observed reflections	204 354, 40 498, 12 714
No. of independent and observed main reflections	3649, 2127
No. of independent and observed first-order satellites	7500, 4402
No. of independent and observed second-order satellites	7537, 3246
No. of independent and observed third-order satellites	7575, 1809
No. of independent and observed fourth-order satellites	7301, 843
No. of independent and observed fifth-order satellites	6936, 287
Criterion for observed reflections	$I \geq 2\sigma(I)$
$R_{int,all}$, $R_{int,obs}$	0.085, 0.049
$R_{int,all}$, $R_{int,obs}$ (main reflections)	0.032, 0.027
$R_{int,all}$, $R_{int,obs}$ (first-order satellite reflections)	0.066, 0.051
$R_{int,all}$, $R_{int,obs}$ (second-order satellite reflections)	0.197, 0.115
$R_{int,all}$, $R_{int,obs}$ (third-order satellite reflections)	0.525, 0.212
$R_{int,all}$, $R_{int,obs}$ (fourth-order satellite reflections)	0.907, 0.270
$R_{int,all}$, $R_{int,obs}$ (fifth-order satellite reflections)	1.360, 0.322
θ_{max} (°)	24.59

Computer programs used: *X-AREA* (Stoe & Cie, 2002), *NADA* (Schönleber *et al.*, 2001), *JANA*2000 (Petricek & Dusek, 2003).

The data collection was carried out using a Stoe IPDS II diffractometer, with a 0.5 mm collimator and sealed X-ray tube radiation. To better evaluate strong and weak reflections, three consecutive measurements were performed with the same measurement strategy but with different exposure times for each frame (M1 with 15 min, M2 with 7 min and M3 with 3 min). Details of these measurements are given in Table 2. In measurement M1, satellite reflections up to fifth order were

observed; in M2 and M3, satellite reflections were observed up to fourth and third orders, respectively. During intensity integration with the *X-AREA* software (Stoe & Cie, 2002) all overlapped reflections were rejected. The reflections of the three data sets were merged to a single set using the program *JANA*2000 (Petricek & Dusek, 2003). In this process, the data sets were rescaled on the basis of reflections with $I > 10\sigma(I)$. Crystal data and details concerning data collection are listed in Table 3. The lattice and modulation-vector parameters were refined with the program *NADA* (Schönleber *et al.*, 2001).

2.3. Unit-cell and modulation-vector parameters at low temperature

To detect possible phase transitions, DSC (differential scanning calorimetry) measurements with a Mettler Toledo STAR^e system (Mettler Toledo, 2000) were performed in the temperature range between room temperature and liquid nitrogen. No anomalies and discontinuities could be detected in the DSC traces.

This result was confirmed by X-ray diffraction experiments, from which the evolution of the lattice and modulation-vector parameters were studied in the temperature range $125 \leq T \leq 295$ K in steps of $\Delta T = 10$ K. No phase transition could be detected; the cell and modulation parameters changed continuously with temperature. The temperature-dependent measurements were performed with a Mar IP instrument (Marresearch, 1998), with synchrotron radiation, at the Swiss–Norwegian Beam Line (SNBL) at the European Synchrotron Radiation Facility (ESRF). The goal of these measurements was not to extract intensities for structure analysis but to refine the lattice and modulation-vector parameters. Therefore, it was not necessary to perform complete data-set measurements. Instead, two oscillation ranges were measured ($0 \leq \varphi \leq 10^\circ$ and $90 \leq \varphi \leq 100^\circ$, both with an increment of $\Delta\varphi = 1^\circ$). Both oscillation ranges were measured successively for each temperature. The peak-finding routine of *CrysAlis RED* (Oxford Diffraction, 2001) yields about 1270 peaks for each temperature, of which ∼340 could be indexed as main reflections. The unit-cell and modulation-vector parameters were refined with the program *NADA* (Schönleber *et al.*, 2001). Approximately 560, 290 and 80 peaks could be indexed as first-, second- and third-order satellite reflections, respectively (because the peak-finding routine applies a certain threshold looking only for 'strong' intensities, main reflections and satellite reflections of lower but not higher order are found). The differences in the absolute numbers of peaks for each temperature can be explained by a change in intensity of the incident beam (synchrotron radiation) and a change of the background for different temperatures.

In the given temperature range, the values of the lattice parameters decrease as expected. In contrast, the modulation-vector parameters are not influenced by temperature. Within the precision of the measurement, all the values of all three parameters remain constant (graphical presentations of the temperature dependence of the volume and of the modulation-vector parameters α and γ are given as supplementary material[1]).

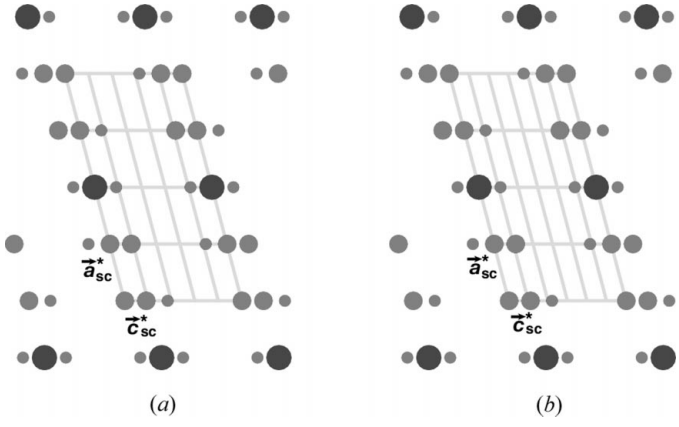

Figure 3
A schematic drawing of the diffraction pattern, showing the main reflections and satellite reflections up to fourth order. It can be seen that, with respect to $\mathbf{c}^*$, (*a*) the 3×5 supercell approximation is slightly too large and (*b*) the 3×6 approximation is slightly too small for an exact indexation of the higher-order satellite reflections by only three indices *hkl*.

3. Structure determination

3.1. Structure solution

Every attempt to solve the structure of quininium (*R*)-mandelate in an average structure by using only the intensities of the main reflections failed. This result might be explained by the occurance of strong modulations that make any average structure chemically meaningless. The presence of a strong modulation is indicated by the presence of satellite reflections up to higher orders. In addition, the lower-order satellite reflections show strong intensities with respect to the main reflections (Fig. 2 and Table 2).

Therefore, a superstructure approximation had to be obtained in order to initiate the structure refinement. The structure of quininium (*R*)-mandelate has been solved independently in both a 3×5 and a 3×6 superstructure approximation based on the respective supercell approximations (Fig. 3). These two approximations are possible because the distance between the main and third-order satellite reflections along $\mathbf{c}^*$ is $(1 - 3 \times 0.2713) = 0.1861$, *i.e.* intermediate between $1/6 = 0.1667$ and $1/5 = 0.2000$.

The relation between the unit-cell parameters of the modulated structure and those of the supercell approximations in direct space is given by

$$(\mathbf{a}_{sc}, \mathbf{b}_{sc}, \mathbf{c}_{sc}) = (\mathbf{a}, \mathbf{b}, \mathbf{c})\underline{\mathbf{P}}, \qquad (1)$$

where

$$\underline{\mathbf{P}}_{3\times5} = \begin{pmatrix} 3 & 0 & 4 \\ 0 & 1 & 0 \\ 0 & 0 & 5 \end{pmatrix} \quad \text{and} \quad \underline{\mathbf{P}}_{3\times6} = \begin{pmatrix} 3 & 0 & 5 \\ 0 & 1 & 0 \\ 0 & 0 & 6 \end{pmatrix}.$$

[1] Supplementary data for this paper are available from the IUCr electronic archives (Reference: SN5002). Services for accessing these data are described at the back of the journal.

Table 4
Details of the superstructure approximation refinements.

Superstructure approximation	3 × 5	3 × 6
a, b, c (Å)	19.842 (9), 18.552 (7), 50.674 (23)	19.842 (9), 18.552 (7), 61.106 (24)
β (°)	77.60 (6)	76.39 (5)
Z'	15	18
Range of h, k, l	$-23 \Rightarrow h \Rightarrow 23$ $-21 \Rightarrow k \Rightarrow 21$ $-27 \Rightarrow l \Rightarrow 59$	$-23 \Rightarrow h \Rightarrow 22$ $-21 \Rightarrow k \Rightarrow 21$ $-34 \Rightarrow l \Rightarrow 71$
$2\theta_{max}$ (°)	49.20	49.23
No. of measured, unique and observed reflections	40498, 22521, 12720	40498, 22521, 12720
Criterion for observed reflections	$F_o > 4\sigma(F_o)$	$F_o > 4\sigma(F_o)$
No. of parameters	4726	5671
No. of restraints	1290	1548
R_{all}, R_{obs}, wR	0.170, 0.046, 0.098	0.167, 0.043, 0.087
GoF	0.762	0.748
$\Delta\rho_{max}$, $\Delta\rho_{min}$ (e Å^{-3})	0.24, −0.18	0.21, −0.23

Computer programs used: *DIRDIF*96 (Beurskens *et al.*, 1996), *SHELXL*97 (Sheldrick, 1997).

In reciprocal space, $\mathbf{a}^*_{sc}$ was chosen to lie almost along the modulation vector $\mathbf{q}$, whereas $\mathbf{b}^*_{sc} = \mathbf{b}^*$ and $\mathbf{c}^*_{sc} = \mathbf{c}^*/n$ ($n = 5$ and 6).

The intensities from the measured raw images were extracted in the superspace model using four indices, *hklm*, and then transformed into the *hkl* parameters of the three-dimensional models. Because only satellite reflections of lower order were used, the transformation $hklm \Rightarrow hkl$ is unambiguous.

For both superstructure approximations, the space group is $P2_1$. Because the 15 and 18 formula units in the asymmetric units of, respectively, the 3 × 5 and a 3 × 6 superstructure approximations (*i.e.* there are 15 or 18 quininium cations together with 15 or 18 mandelate anions in the asymmetric unit) deviate only slightly from a periodic arrangement, neither direct methods nor Patterson functions were successful in the first attempt. This initial lack of success was a result of the super- and/or pseudosymmetry associated with the large number of similarly positioned molecules in the asymmetric unit. It also became clear after some attempts at structure solution that it was necessary from the very first to restrain the interatomic distances. The aim of these restraints was to maintain the bond lengths and angles, and the complete geometry of the molecules, within chemically plausible ranges. Appropriate values for the interatomic distances and angles were found by searching the Cambridge Structural Database (CSD; Allen, 2002; CCDC, 2000). Without these restraints, the calculated molecules were not stable and broke apart during successive steps of expanding and completing the structure. With an alternate use of *DIRDIF*96.3 (Beurskens *et al.*, 1996) and *SHELXL*97 (Sheldrick, 1997) it was thus possible to use some chemical knowledge, *i.e.* the shape and geometry of the quinine molecule, to obtain an initial structural model. For the refinements, the ideal supercell parameters and their respective errors derived from (1) with the lattice parameters of the reference structure were applied. The asymmetric units of the two resulting superstructure approximations are presented in Fig. 4 and details of their refinements in Table 4. H atoms were placed at calculated positions (*SHELXL*97; Sheldrick, 1997) and treated as riding atoms. As a consequence of the approximate character of the 3 × 5 superstructure, 46 atoms could be split. In the 3 × 6 superstructure approximation, 61 atoms could be split and 20 atoms were non-positive definite (the splitting of the atoms was not performed).

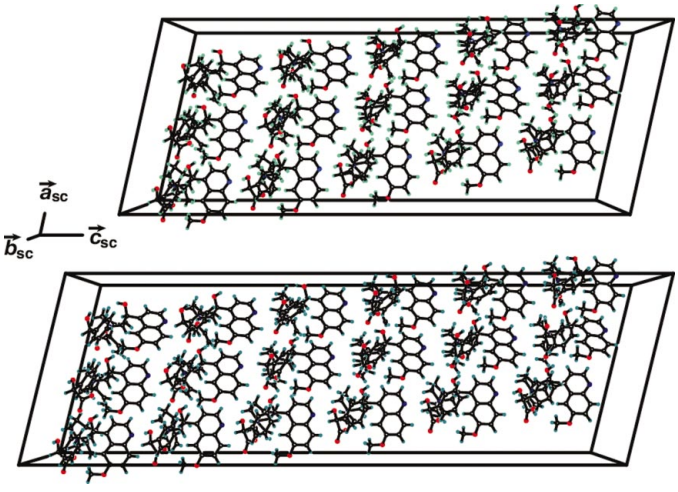

Figure 4
The 3 × 5 (above) and 3 × 6 (below) superstructure approximations, showing, respectively, the 15 and 18 formula units in the asymmetric units.

3.2. Modulation in the superstructure approximations

The fractional coordinates, x, y, z, of one formula unit of the superstructures were transformed into the unit cell of the modulated structure. The aim was to use these coordinates as starting values for the fractional coordinates of the reference structure. This model (several different formula units were chosen) did not allow us to find good starting values for the atomic modulation functions (atomic surfaces) for the refinement, *i.e.* this structure model did not allow a stable refinement of the modulation functions. Hence, additional information had to be extracted from the superstructure

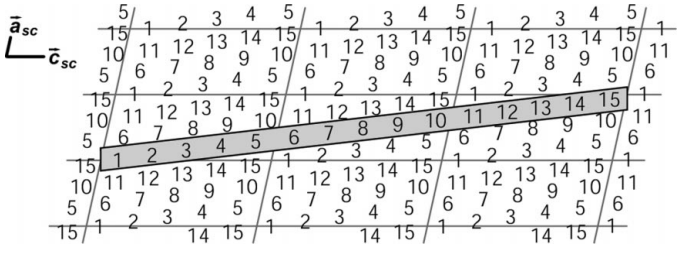

Figure 5
The periodicity of the unit cell in the 3 × 5 superstructure approximation of quininium (*R*)-mandelate (schematic drawing) in the ($\mathbf{a}_{sc}$, $\mathbf{c}_{sc}$) plane. The molecules are replaced by numbers from 1 to 15. The sequence extends parallel to the $\mathbf{a}_{sc} + 3\mathbf{c}_{sc}$ direction.

approximations in order to refine the structure in the (3+1)-dimensional superspace.

In both superstructure approximations, the molecules in the asymmetric unit are arranged along three parallel lines (Fig. 4). Each line contains five (six) molecules forming periodically repeating rows of 15 (18) molecules parallel to the $\mathbf{a}_{sc} + 3\mathbf{c}_{sc}$ direction (Fig. 5). These rows are denoted 'sequences' in the following.

3.2.1. Qualitative information about the modulation. The 15-molecule sequence of the 3×5 superstructure approximation is presented in Fig. 6. For clarity, H atoms have been omitted and only the bicyclic flat quinoline moieties, the vinyl groups of the quininium cations and the phenyl rings of the mandelate anions are shown in the sequences. The displacive modulations of the single atoms lead to an undulation and displacement of the moieties along the sequence of the 15 molecules with respect to their neighbours. No severe distortion of the molecular parts could be detected, this lack of distortion being due to the restraints for interatomic distances and angles.

3.2.2. Quantitative information on the modulation. The sequence (of 15 or 18 formula units) is periodically repeated in the three-dimensional superstructure approximations and hence might be interpreted as the structural basic unit. The 15 (18) formula units and the single atoms in these formula units can be described as a function of their position in the sequence, *i.e.* an additional coordinate, $\xi_{3\times5} = 0, \frac{1}{15}, \frac{2}{15}, \frac{3}{15}, \ldots$ or $\xi_{3\times6} = 0, \frac{1}{18}, \frac{2}{18}, \frac{3}{18}, \ldots$, is introduced, with $0 \leq \xi < 1$ for each ion or atom. To obtain quantitative information, the fractional coordinates, x, y, z, of each single atom were fitted along the 15 (18) formula units by harmonic functions, using the program *IGOR PRO* 4.0 (WaveMetrics, 2000), as a function of ξ. This procedure allows the derivation not only of new starting values for the fractional coordinates, but also of starting values for the parameters of the displacive modulation functions of the single atoms.

For the purpose of curve fitting, the equation

$$\begin{aligned} f(\xi) = X &+ A_1 \cos(2\pi \times 1\xi) + B_1 \sin(2\pi \times 1\xi) \\ &+ A_2 \cos(2\pi \times 2\xi) + B_2 \sin(2\pi \times 2\xi) \\ &+ A_3 \cos(2\pi \times 3\xi) + B_3 \sin(2\pi \times 3\xi) \end{aligned} \quad (2)$$

was applied. This expression is a Fourier expansion, *i.e.* a continuous function generated by the superposition of harmonic waves of higher order. In the present case, harmonic waves of first-, second- and third-order were applied. X represents the fractional coordinates x, y, z, and A_i and B_i are the modulation parameters of the first-, second- and third-harmonic wave.

As an example, the results of curve fitting for the fractional coordinates of atom C21 in the bicyclic flat quinoline moiety are presented in Fig. 7. The undulating character of the displacive modulation can be seen clearly for all three coordinates.

Note that the shifts $\Delta x \simeq 0.20$, $\Delta y \simeq 0.05$ and $\Delta z \simeq 0.07$ for atom C21 in units of the lattice parameters are equivalent to 1.32, 0.93 and 0.73 Å, thus confirming the assumption of a strong modulation.

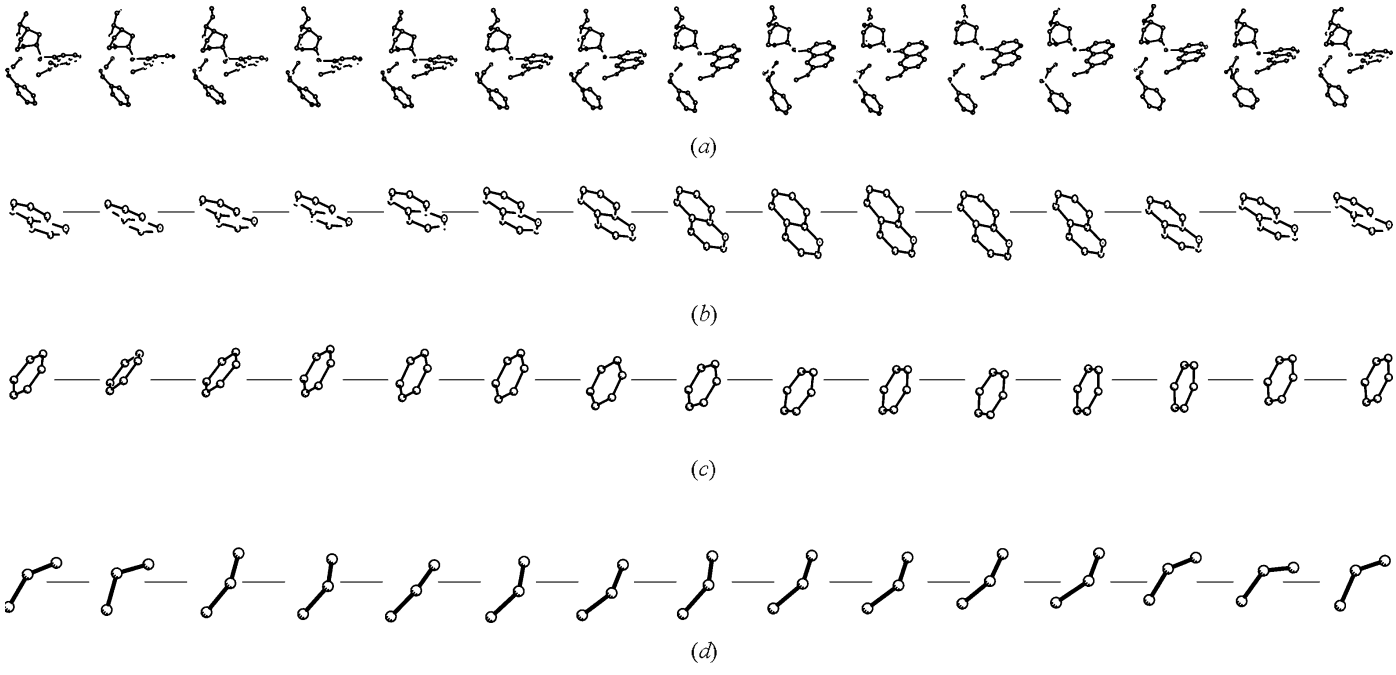

Figure 6
Sequence of the formula units in the 3×5 superstructure approximation of quininium (*R*)-mandelate (only the non-H atoms are shown). For clarity, the orientations and the scaling of (*a*)–(*d*) differ. (*a*) The complete quininium cations and the mandelate anions. (*b*) The quinoline moieties of the quininium cations, showing a strong undulation. (*c*) The phenyl rings of the mandelate anions, showing a slight undulation and some displacement. (*d*) The vinyl groups, showing the two preferred orientations.

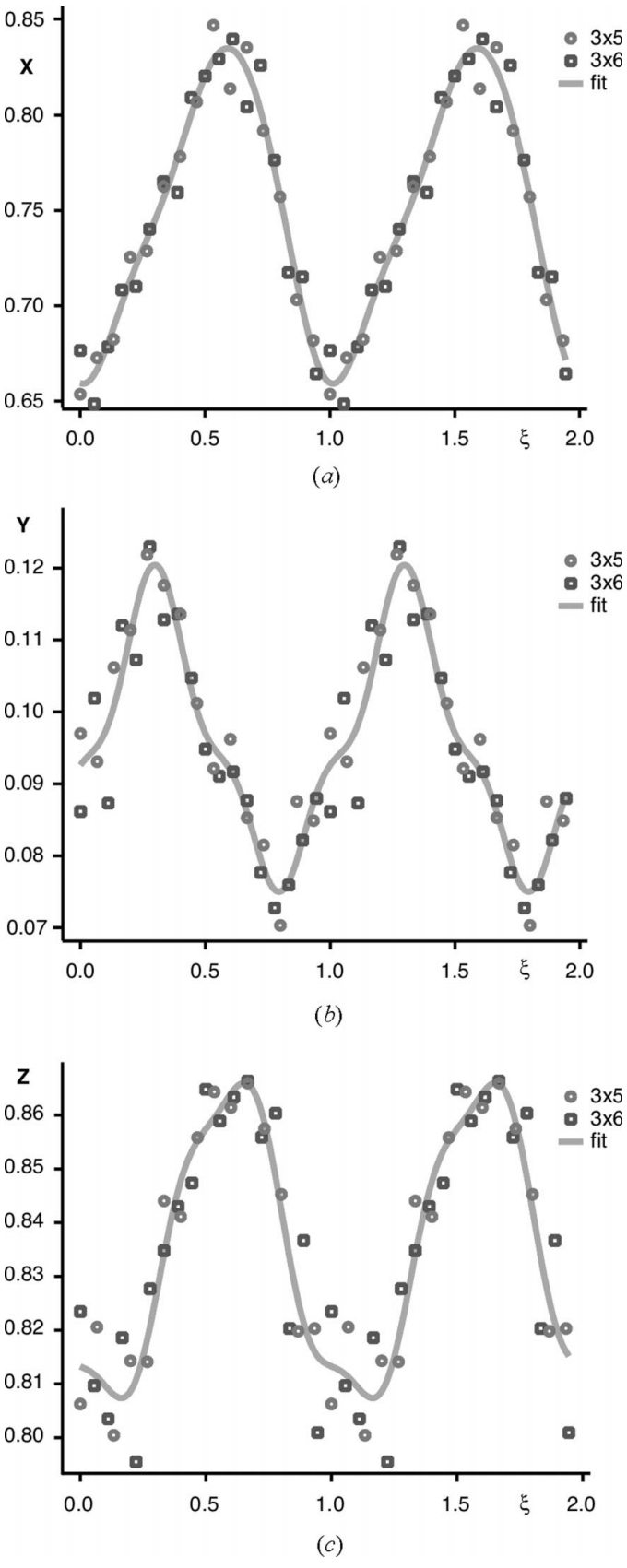

Figure 7
The result of curve fitting on the fractional coordinates (*a*) *x*, (*b*) *y* and (*c*) *z* for atom C21. For clarity, two periods of ξ are shown along the horizontal axes.

3.3. Refinement in superspace

The refinement of the structure in (3+1)-dimensional superspace was performed with the program *JANA*2000 (Petricek & Dusek, 2003). The numbers given in this section, which describes the refinement process, refer to a refinement based on the observed main and satellite reflections up to fifth order. Because of the numerous parameters to be refined, the observation criterion was lowered to $I \geq 2\sigma(I)$, yielding 12714 instead of 9773 observed reflections. The restraints presented in §3.1 were applied again during the refinement process, in order to guarantee chemically reasonable bond lengths and angles.

3.3.1. Individual atoms. In the starting model, the fractional coordinates of the atoms were refined, together with the isotropic atomic displacement parameters (ADPs) and a displacive modulation for all atoms (including H atoms), which was described by three harmonic waves. For the initial values of the fractional coordinates and of the displacive modulation parameters, the values obtained using (2) were adopted. After introducing anisotropic ADPs for the non-H

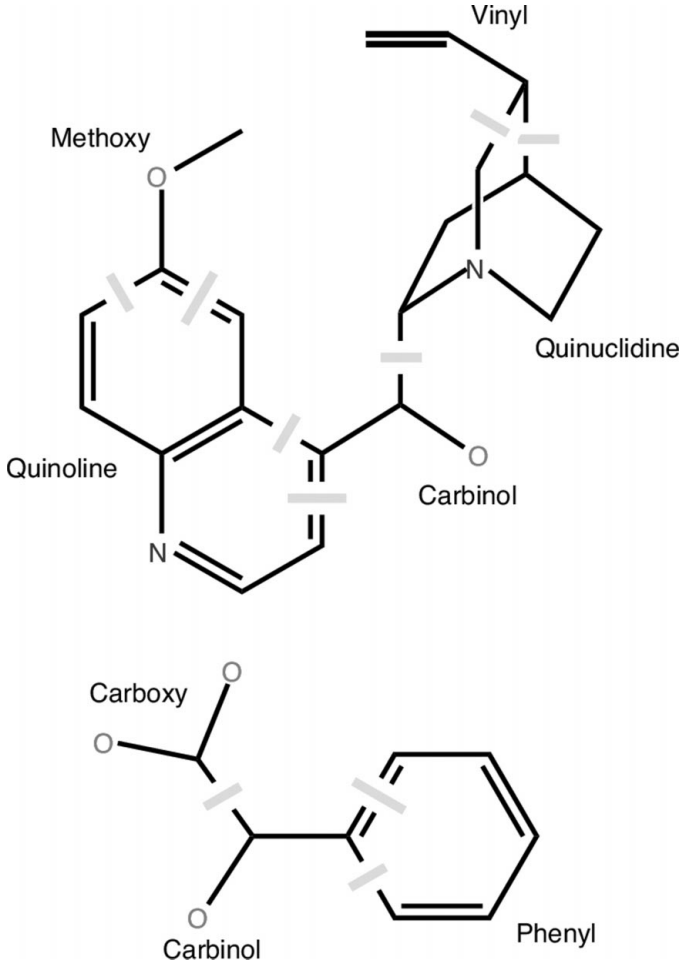

Figure 8
The splitting of the quininium cation (top) and mandelate anion (bottom) into molecular fragments (for clarity, only the non-H atoms are shown). These molecular entities serve as rigid bodies, with common displacive modulation functions for all their atoms.

atoms, a total number of 1618 parameters had to be refined. The positions of the H atoms were refined with restrained bond lengths and angles. The isotropic displacement parameters, U_{iso}^{calc}, of the H atoms were calculated from the U^{ij} values of the bonded atoms, as illustrated by (3) for atom H03 bonded to atom C03

$$U_{iso}^{calc}[H03] = 0.396U^{11}[C03] + 0.396U^{22}[C03] + 0.396U^{33}[C03]. \quad (3)$$

For the two H atoms bonded to atoms O12 and O29 (the hydroxy groups), as well as for the three H atoms bonded to atom C24 (the methoxy group), the value 0.495 was applied instead of 0.396. Equation (3) fixes the U_{iso}^{calc} values of the H atoms to ~1.2 (1.5 for the hydroxy and methoxy groups) times the U_{eq} (Sheldrick, 1997) of the carrier atoms (assuming that U_{eq} can be approximated as $U^{11}/3 + U^{22}/3 + U^{33}/3$). The general use of constraints/restraints to control the refinement of difficult structures has been described by Watkin (1994). The highest and lowest peaks in the difference-Fourier map were 0.81 and −1.16. The goodness of fit (GoF) was 2.82, and

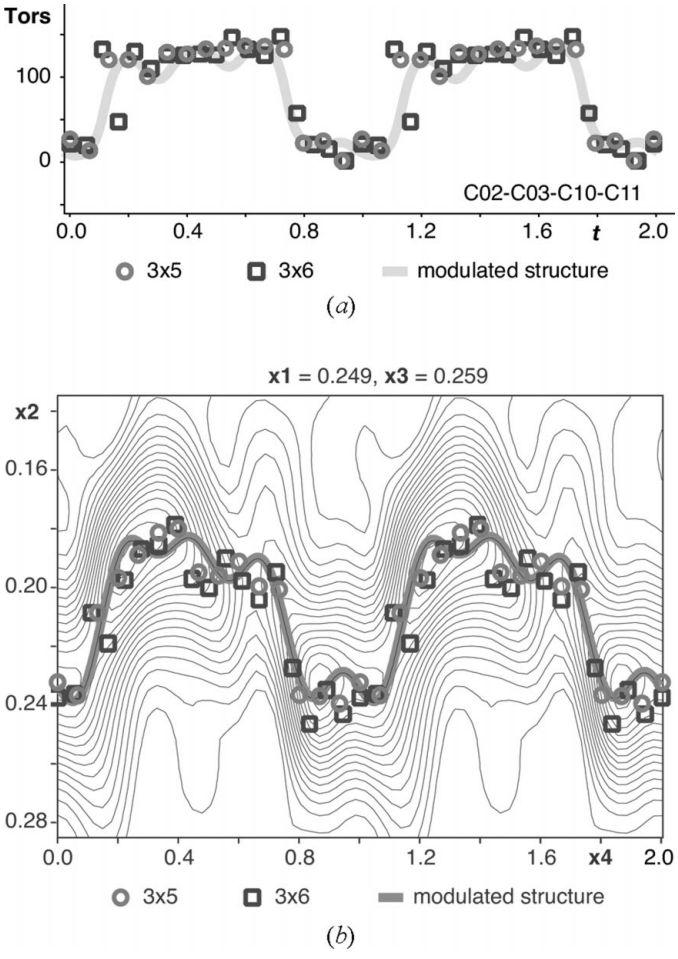

Figure 9
Orientation of the vinyl group. (*a*) Torsion angle C02—C03—C10—C11 as a function of the modulation parameter *t*. (*b*) Fourier map for atom C10 in the x_2–x_4 plane, refined in (3+1)-dimensional superspace. For clarity, two periods are shown along the fourth dimension. In addition, the values found in the superstructure approximations are superimposed.

R and *wR* for all observed reflections were 0.1185 and 0.1201. The ratio between the number of refined parameters and the number of used reflections was 7.9.

A strong displacive modulation also often induces modulation of the ADPs as a response to the varying environment of the atoms. Hence a modulation of the ADPs was introduced, in addition to the positional modulation for all non-H atoms. Because of the already high number of parameters, only one harmonic wave could be added. Nevertheless, the resulting statistical parameters improved. The total number of parameters was 2038, with a ratio of 6.3 between the number of refined parameters and the number of used reflections. The highest and lowest peaks in the difference-Fourier map were 0.75 and –0.82. The GoF decreased to 2.55, and *R* and *wR* for all observed reflections were 0.107 and 0.107.

This model with individually refined atoms requires the refinement of a very large number of parameters. For example, each H atom requires 21 parameters, *viz.* three parameters for the fractional coordinates and 18 parameters for the three waves of positional modulation. There were more then 40 correlations greater than 0.9 between parameters, these correlations being mainly related to H atoms. The refinement did not converge completely but did oscillate between several values for some H-atom modulation parameters.

3.3.2. Molecular fragments as rigid bodies. In order to overcome the large number of parameters and to treat the H atoms properly, molecular fragments were introduced (Fig. 8). Each is assumed to act as a rigid body, which means that the atoms of each molecular fragment are refined with individual fractional coordinates (x, y, z), individual anisotropic ADPs (U^{ij}) and individual modulation of the anisotropic ADPs but with a common displacive modulation. Besides, decreasing the number of parameters, these molecular fragments also have the advantage of preserving the shape of each single entity.

Following the introduction of three harmonic waves for positional modulation for each molecular fragment and one harmonic wave for the modulation of the anisotropic ADPs of the non-H atoms, a total of 1120 parameters had to be refined, the ratio between the number of refined parameters and the number of reflections used being 11.4. Therefore, a second harmonic wave for the modulation of the ADPs of the non-H atoms was included. Every attempt to introduce TLS tensors and their modulations instead of individual ADPs for the atoms (assuming that all atoms of the rigid body move in phase) resulted in unacceptable ADPs for several atoms. Hence the TLS refinement was abandoned.

The total number of parameters was 1540, the ratio between the number of refined parameters and the number of reflections used being 8.3. The highest and lowest peaks in the difference-Fourier map were 0.71 and −0.74. The GoF decreased to 2.29, and *R* and *wR* for all observed reflections were 0.100 and 0.098.

After introducing a fourth-harmonic wave for the displacive modulation for all molecular fragments, the *R* values for the main reflections improved by ~0.6% and those of the satellite reflections improved by 0.8, 2.0, 5.1, 7.2 and 2.2%. The total number of parameters was 1636, the ratio between the number

Table 5
Refinement data.

Refinement on	F
R_{all}, wR_{all}	0.160, 0.079
R_{obs}, wR_{obs}	0.074, 0.072
R_{obs}, R_{all}, wR_{all} (main reflections)	0.047, 0.081, 0.057
R_{obs}, R_{all}, wR_{all} (first-order satellite reflections)	0.066, 0.112, 0.068
R_{obs}, R_{all}, wR_{all} (second-order satellite reflections)	0.092, 0.195, 0.092
R_{obs}, R_{all}, wR_{all} (third-order satellite reflections)	0.172, 0.384, 0.203
S_{obs}, S_{all}	1.78, 1.25
No. of restraints	90
No. of parameters	1636
Weighting scheme	$w = [\sigma^2(F) + (0.02F)^2]^{-1}$
$(\Delta/\sigma)_{max}$	0.0002
$\Delta\rho_{max}$, $\Delta\rho_{min}$ (e Å^{-3})	0.88, −0.81
Extinction correction	Gaussian isotropic type I

Computer programs used: *JANA*2000 (Petricek & Dusek, 2003).

of refined parameters and the number of used reflections being 7.8. The highest and lowest peaks in the difference-Fourier map were 0.57 and −0.53. The GoF decreased to 1.90, and R and wR for all observed reflections were 0.085 and 0.081. In the last refinement cycle, seven correlations (all concerning the displacive modulation of the vinyl group) were larger than 0.9.

3.3.3. Crenel functions for the vinyl groups. From the superstructure approximations (Fig. 6*d*), two preferred orientations can be detected for the vinyl group, but the arrangement of these two orientations along the sequence is not arbitrary. In the 3×5 superstructure approximation, one orientation is adopted by ten successive groups, the other by the remaining five groups. In the 3×6 superstructure approximation, the frequency is 12 to 6. Consequently, the C02—C03—C10—C11 torsion angle shows two preferred values, ∼10 and 120°. These values can be reproduced by the continuous modulation functions, as shown in Fig. 9, which also shows the Fourier map of atom C10, with its modulation function.

In order to improve the model for the two different preferred orientations, discontinuous crenel functions (Petricek *et al.*, 1990, 1995; van der Lee *et al.*, 1994) for the vinyl group were introduced. The aim is to refine the positional modulation generated by the two preferred orientations as occupational modulation of each orientation. In order to take into account the different chemical environments of the atoms, two independent crenel functions, one for each position, were introduced.

A crenel function is defined by its width, Δx_4, and its centre, x_4^o. As starting values for the widths of the two functions, 1/3 and 2/3 were chosen. The values for the centres of the functions were taken from the Fourier maps. Assuming that the displacive modulation functions are modelled by crenel functions, exactly one and only one crenel function must be defined for each value of t. Therefore, gaps and overlaps in the crenel functions are forbidden [in this context it is important to refer to the modulation parameter, t, and not to the fractional coordinate, x_4, because the crystals are defined as cuts of the (3+1)-dimensional superspace with the same t and not the same x_4]. Therefore, the sum of the widths has to be 1: $\Delta x_4^b = 1 - \Delta x_4^a$. In addition, the centres of the two crenel functions, x_4^o or preferably t^o, have to be separated by $\Delta x_4^a/2$ and $\Delta x_4^b/2$: $t^{o,a} = t^{o,b} + \Delta x_4^a/2 + \Delta x_4^b/2$. Applying the relation between t and x_4 [$t = x_4 - \mathbf{qr}$ (*International Tables for Crystallography*, 1992, Vol. C, pp. 797–835)], we obtain for the centres of the crenel functions $x_4^{o,a} = x_4^{o,b} + 1/2 - \mathbf{qr}_b + \mathbf{qr}_a$.

After superposing two harmonic waves for displacive modulation on the crenel functions, the widths of the two functions refined to 0.61 and 0.39. This model slightly reduced the number of parameters but did not substantially improve the fit of the refinement. The total number of parameters was 1605, the ratio between the number of refined parameters and the number of used reflections being 7.9. The highest and lowest peaks in the difference-Fourier map were 0.56 and −0.53. The GoF was 1.91, and R and wR for all observed reflections were 0.085 and 0.081. Two correlations (for the positions of atoms H10 and H11 of the smaller crenel function) were larger than 0.9 in the last refinement cycle. The refinement did not converge completely but did oscillate between two values for one parameter concerning the modulation of the smaller crenel function.

4. Result and discussion

In this section, the discussion of the structure is based on the model with continuous modulation functions, as described in §3.3.2. The model applying crenel functions was not retained because it improved the fit for neither the refinement nor the bond lengths and angles in the structure. In addition, a discontinuity in the displacive modulation function might produce a strong modulation of the ADPs with maxima at these discontinuities (Perez-Mato *et al.*, 2003). These maxima could not be detected in the present structure.

In the last steps of refinement, the fourth- and fifth-order satellite reflections were discarded because of their large R_{int} values and because their total number is not significantly large (Tables 3 and 5). This final refinement was based on all main and satellite reflections up to third order, yielding 26261 reflections, the ratio between the number of refined parameters and the number of reflections used being 16.1. In addition, all restraints concerning bond lengths and angles were removed. As a consequence, the covalent bond lengths for some H atoms (H03, H10, H11*A*, H11*B*, H28, H29 and H35) were not chemically reasonable, and therefore the restraints relating to the H-atom positions were retained. Even so, for the H atoms in the vinyl group (H03, H10, H11*A* and H11*B*) the values are still not chemically valid and the distance for atom H28 is still slightly too large. The problem of H-atom treatment could not be resolved by applying crenel functions for the vinyl group (the values were acceptable for the larger function but not for the smaller). For all other H atoms, the covalent bond distances are reasonable.

In the last refinement cycle, 14 correlations (all concerning the displacive modulation of the vinyl group) exceeded 0.9. The final residual parameters of the refinement are given in Table 5, and the atomic coordinates and equivalent isotropic displacement parameters are given in the supplementary

Table 6
Torsion angles (°) in the quininium cation compared with those found in quininium (*S*)-mandelate (Gjerløv & Larsen, 1997*b*).

	Mean	Min.	Max.	$\lvert\Delta_{\mathrm{Max-Min}}\rvert$	Quininium (*S*)-mandelate
τ_1	−17.7 (8)	−24.5 (8)	−10.4 (8)	14.1	−24
τ_2	−74.7 (7)	−79.3 (7)	−68.8 (7)	10.5	−82
τ_3	45.6 (7)	39.8 (7)	53.0 (7)	13.2	39
τ_4	−78.0 (5)	−84.0 (5)	−70.6 (5)	13.3	−84

material. The anisotropic ADPs with their modulation parameters, the molecular modulation parameters, the covalent bond lengths and angles, and the restraints applied for the H-atom positions are given as supplementary material.

With the exception of the bond lengths and angles (see supplementary data) in the vinyl group, all the mean bond lengths and angles of the quininium cation and of the mandelate anion are in very good agreement with the values published for quininium (*S*)-mandelate (Gjerløv & Larsen, 1997*b*). The values for the vinyl group are not chemically reasonable. They exhibit significant changes with the modulation along the internal dimension *t* and reflect the difficulties of properly describing the modulation with two orientations in the refinement. For the quininium cation, the bond lengths and angles between atoms of the same molecular fragment remain constant within the standard uncertainties along the fourth dimension *t* [*e.g.* for the N01—C08 bond length, the mean is 1.51 (2) Å, with a minimum of 1.50 (2) Å and a maximum of 1.52 (2) Å], but vary slightly between atoms of different molecular fragments [*e.g.* for the C08—C09 bond length, the mean is 1.54 (3) Å, with a minimum of 1.49 (3) Å and a maximum of 1.59 (3) Å]. The same is true of the mandelate anion, but here a slight variation can also be observed for bonds between atoms of the same molecular fragment. The quininium cation as a whole seems to be more rigid along the internal dimension than the mandelate anion.

With three N—C bond lengths between 1.50 and 1.51 Å in the quinuclidine moiety, we can confirm the protonation of the N01 atom (Oleksyn *et al.*, 1978; Larsen *et al.*, 1993; Oleksyn & Serda, 1993; Gjerløv & Larsen, 1997*b*). For the unprotonated case, as in the free bases, we would expect a smaller value, of ∼1.48 Å (Oleksyn *et al.*, 1979; Oleksyn, 1982; Kashino & Haisa, 1983; Pniewska & Suszko-Purzycka, 1989). The

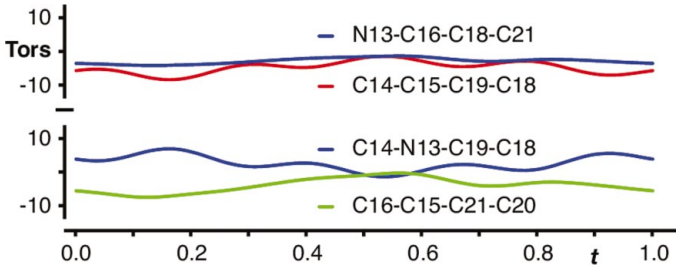

Figure 10
Flat torsion angles in the quinoline moiety of the quininium cation, showing a planar configuration.

Table 7
Torsion angles (°) in the mandelate anion of quininium (*R*)-mandelate compared with those found in quininium (*S*)-mandelate (Gjerløv & Larsen, 1997*b*).

Different signs are a result of a different absolute configuration at the chiral atom C28.

	Mean	Min.	Max.	$\lvert\Delta_{\mathrm{Max-Min}}\rvert$	Quininium (*S*)-mandelate
τ_5	27.7 (9)	3.6 (10)	46.9 (9)	43.3	−5
τ_6	169.4 (9)	145.5 (9)	195.5 (9)	50.0	−167
τ_7	−73.3 (8)	−97.1 (8)	−55.3 (8)	41.8	70.32

deprotonation is also reflected in the C—O bond lengths of the carboxy group. However, the C25—O26 bond is slightly longer than the C25—O27 bond, indicating a probable hydrogen bond with the deprotonated H01 atom (see below). The C14—N13—C22 bond angle [mean 116.0 (15)°, minimum 115.3 (16)° and maximum 117.0 (15)°] is clearly smaller than

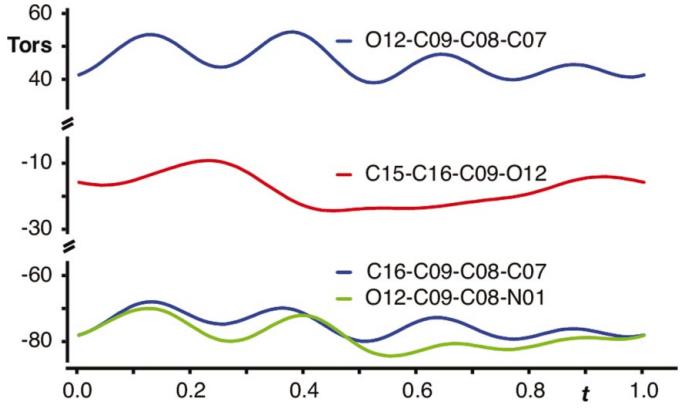

Figure 11
Torsion angles in the quininium cation as a function of the internal space dimension.

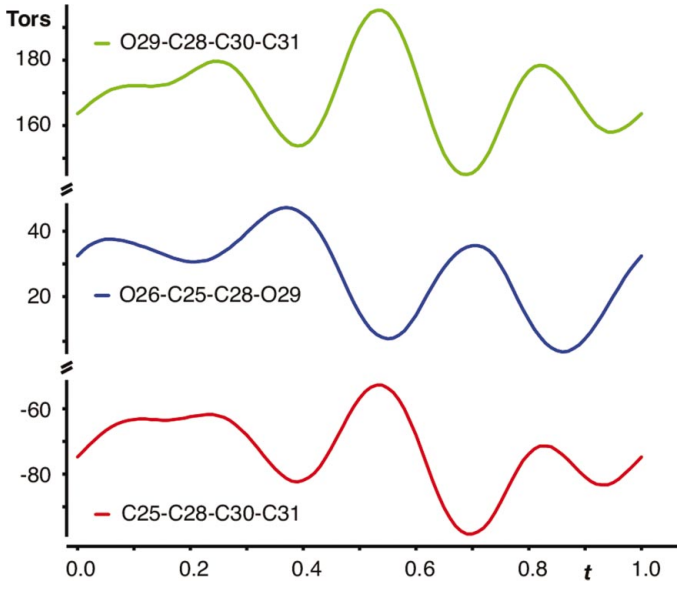

Figure 12
Torsion angles in the mandelate anion along the fourth dimension, *t*.

Table 8
Hydrogen-bonding geometry (Å, °) .

Minimum and maximum values that are printed in bold do not correspond to chemically acceptable values for moderate hydrogen bonds (Jeffrey, 1997) and indicate that the hydrogen bond is not present over the complete *t* range.

	D—H			H···*A*			*D*···*A*			*D*···*A*		
Bond	Mean	Min.	Max.	Mean	Min.	Max.	Mean	Min.	Max.	Mean	Min.	Max.
N01—H01 ··· O26	0.92 (3)	0.91 (3)	0.93 (3)	1.81 (5)	1.58 (5)	2.00 (5)	2.65 (4)	2.46 (4)	2.80 (4)	153 (4)	143 (4)	174 (4)
O12—H12··· O26^{i}	0.86 (5)	0.86 (5)	0.88 (5)	2.35 (6)	1.70 (7)	**3.29 (6)**	2.90 (5)	2.51 (5)	**3.70 (5)**	127 (4)	**92 (4)**	158 (5)
O12—H12···O27^{i}	0.86 (5)	0.86 (5)	0.88 (5)	2.37 (5)	1.69 (6)	**3.12 (5)**	3.18 (4)	2.50 (5)	**3.92 (4)**	158 (4)	142 (4)	179 (4)

Symmetry code: (i) 1 + *x*, *y*, *z*.

120°, thus indicating that this second N atom in the quininium cation is not protonated but possesses a free electron pair pushing the N atom towards the centre of the quinoline ring.

Because of its aromatic character, the quinoline double ring shows a planar conformation. The torsion angles are all close to the expected value of 0° and they show a small deviation along *t*, which might be due to the undulation of this molecular fragment (Fig. 10).

The screwed conformation for the quinuclidine moiety, with a twist angle of ∼8–13° as reported for the non-modulated structures (Oleksyn *et al.*, 1978; Kashino & Haisa, 1983; Oleksyn & Serda, 1993), cannot be verified. The methoxy group, which is appended to the quinoline moiety at atom C19, follows the quinoline undulation. Atoms O23 and C24 are maintained in the plane defined by the quinoline double ring along the internal space as a function of the modulation parameter *t*.

The conformation of the *cinchona* alkaloids and hence of the quininium cation can be described by the four torsion angles τ_1 = C15—C16—C09—O12, τ_2 = C16—C09—C08—C07, τ_3 = O12—C09—C08—C07 and τ_4 = O12—C09—C08—N01. Their absolute values are $\tau_1 \simeq 10$–30°, $\tau_2 \simeq 45$–75°, $\tau_3 \simeq 40$–60° and $\tau_4 \simeq 70$–85°. These torsion angles are quite stable, and no significant influence from the crystalline environment was detected (Oleksyn *et al.*, 1979; Oleksyn, 1980, 1982; Kashino & Haisa, 1983; Suszko-Purzycka *et al.*, 1985; Pniewska & Suszko-Purzycka, 1989). The values found in quininium (*R*)-mandelate are presented in Table 6 and Fig. 11. Here also no significant influence of the modulation is observed; the variation of the angles along the modulation is $|\Delta_{\rm Max-Min}| \simeq 15°$, and the minimum and maximum values are within the ranges found for the non-modulated structures. The values are in good agreement with those of quininium (*S*)-mandelate (Gjerløv & Larsen, 1997*b*).

Similarly, for the mandelate anion, the torsion angles τ_5 = O26—C25—C28—O29, τ_6 = O29—C28—C30—C31 and τ_7 = C25—C28—C30—C31 are illustrated in Table 7 and Fig. 12. In the non-modulated structures, τ_5 corresponds to an almost planar arrangement between the carboxy group and the hydroxy group, the preferred conformation being between 10 and 20°; τ_6 is ∼150°, and τ_7 varies between 70 and 130° (Larsen & Lopez de Diego, 1993; Larsen *et al.*, 1994). However, the variation of the angles along the modulation is rather large ($|\Delta_{\rm Max-Min}| \simeq 45°$). In Figs. 10–12, the same scales are applied. In addition to these large variations, τ_5 is not close to 0°; the hydroxy and carboxy groups are clearly not planar. τ_6 and τ_7 correspond well to the values in quininium (*S*)-mandelate (Gjerløv & Larsen, 1997*b*).

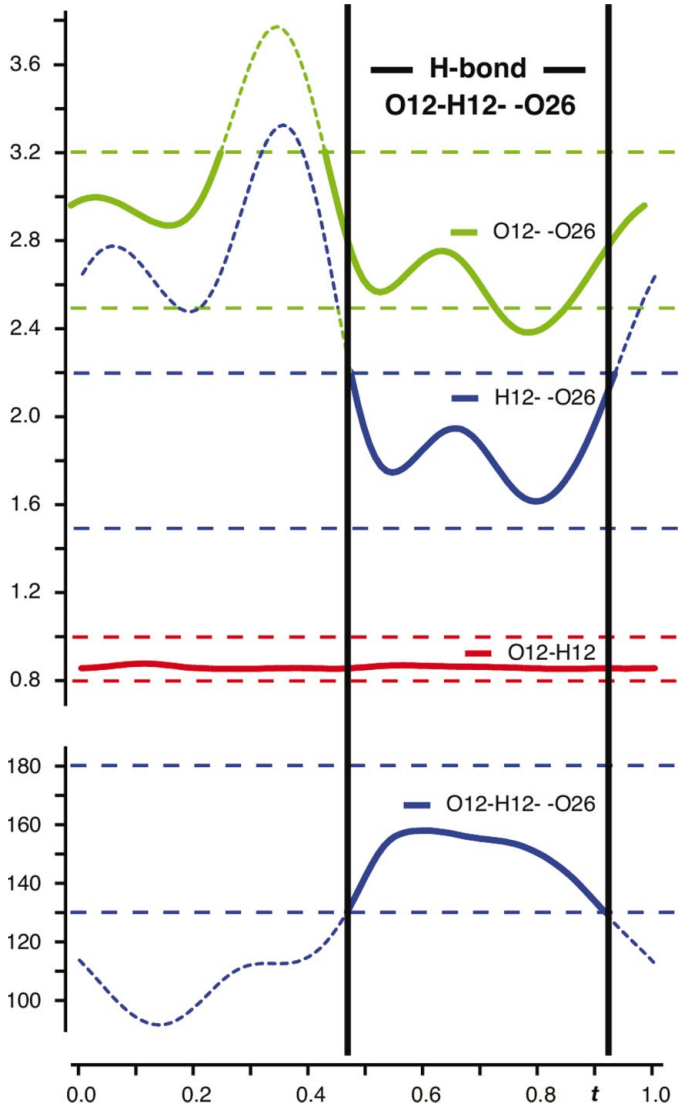

Figure 13
Bond lengths (Å) and angles (°) for the O12—H12···O26(1 + *x*, *y*, *z*) hydrogen bond along the internal space as a function of the modulation parameter *t*. For each value, the following ranges for a moderate hydrogen bond are indicated: *D*—H = 0.8–1.0 Å, H···*A* = 1.5–2–2 Å, *D*···*A* = 2.5–3.2 Å and *D*—H···*A* = 130–180° (Jeffrey, 1997).

The two preferred orientations of the vinyl group with torsion angle τ_8 = C02—C03—C10—C11 have already been discussed in §3.3.3. Owing to the difficulty of properly modelling the modulation of this group, not only the bond lengths and angles but also the anisotropic ADPs of the atoms in the vinyl group are unrealistic (supplementary data). The two preferred values (∼10 and 120°) can be found in the non-modulated structures. In quininium (*S*)-mandelate (Gjerløv & Larsen, 1997*b*), cinchonidinium (*S*)- and (*R*)-mandelate (Gjerløv & Larsen, 1997*a*) and cinchoninium (*S*)-mandelate (Larsen *et al.*, 1993) the torsion angles are $\tau_8 = 114°$, $\tau_8 = 125/128/117°$ and $\tau_8 = 124°$, respectively. In cinchoninium (*R*)-mandelate (Larsen *et al.*, 1993) they are $\tau_8 = -14/9°$. In the non-modulated structures, either one or the other value is present, even in the cases of cinchonidinium (*R*)-mandelate and cinchoninium (*R*)-mandelate, which both have two independent molecules in the asymmetric unit. In the modulated structure of quininium (*R*)-mandelate, both values are present in the same molecule.

There are two possible intramolecular hydrogen bonds, namely O12—H12···N01 in the quininium cation and O29—H29···O26 in the mandelate anion. The latter is present in quininium (*S*)-mandelate, cinchonidinium (*S*)- and (*R*)-mandelate, and cinchoninium (*R*)-mandelate, but not in cinchoninium (*S*)-mandelate (Larsen *et al.*, 1993; Gjerløv & Larsen, 1997*a*,*b*). In the present structure, neither the O12—H12···N01 nor the O29—H29···O26 bond is realized. The absence of the latter is already indicated by the non-planarity of the carboxy–hydroxy moiety (τ_5 = O26—C25—C28—O29 in Table 7 and Fig. 12).

However, two intermolecular hydrogen bonds are present; in the first, the protonated quinuclidinium atom N01 in the quininium cation acts as a donor, via H01, to atom O26 in the carboxy group of the mandelate anion (Table 8). The presence of this hydrogen bond is also reflected in the fact that the C25—O26 bond is slightly longer than the C25—O27 bond. In general, for a deprotonated carboxy group, both distances should be equal.

The second hydrogen bond links the O12 atom of the carbinol group in the quininium cation to atoms O26 and O27 of the carboxy group in the mandelate anion [O12—H12···O26^{i} and O12—H12···O27^{i}; symmetry code: (i) $1 + x$, y, z]. The O12—H12···O26^{i} bond does not exist along the complete t range, as indicated by the minimum and maximum interatomic distances given in Table 8. In Fig. 13 the bond lengths and angles are shown as a function of the modulation parameter t. The hydrogen bond exists only in the range $0.48 \leq t < 0.92$.

Similarly, it can be shown that, in the ranges $0 \leq t < 0.48$ and $0.92 \leq t < 1$ the H12 atom is involved in a hydrogen bond with the O27^{i} atom [symmetry code: (i) $1 + x$, y, z]. Hence this hydrogen bond switches between atoms O26 and O27 along t. Besides the three hydrogen bonds in Table 8, no other hydrogen bond could be detected, *i.e.* no possible bond was found for the O29 atom, neither as a donor nor as an acceptor, or for atom N13 as an acceptor.

5. Conclusion

Because of strong modulation, the approximate structure of quininium (*R*)-mandelate has been solved in two superstructure approximations, with $Z' = 15$ and $Z' = 18$. These two three-dimensional approximations, in which only main and satellite reflections of low-order approximately fit the three-dimensional lattices, can supply a unique starting model for the refinement of the incommensurately modulated structure in (3+1)-dimensional superspace by extracting qualitative and quantitative information about the modulation. In order to treat the H atoms properly and to reduce the number of parameters, molecular fragments were defined. These act as rigid bodies and are refined with common displacive modulation functions. The modulation of the ADPs was refined individually for each non-H atom.

The refinement in superspace has some difficulty in describing the modulation of the vinyl group, which occupies two distinct preferred orientations. The use of discontinuous functions for the description of the displacive modulation, *i.e.* crenel functions, could not improve the fit.

No intramolecular hydrogen bonds could be found. One intermolecular hydrogen bond is stable along the complete t range, and another switches between two possible acceptors as a function of the internal space dimension t. Therefore, the origin of the modulation lies in competition between the conformation of the molecules (intramolecular forces) and the hydrogen-bond motif (intermolecular forces).

The authors thank Anne Mølgaard, née Gjerløv, and Sine Larsen for their information concerning crystal growth and gratefully acknowledge Michal Dusek and Vaclav Petricek for valuable discussions and for help with *JANA*2000. The authors also thank Phil Pattison and the staff of the Swiss–Norwegian Beam Lines (ESRF) for their assistance with the synchrotron measurements. This work was supported by the Swiss National Science Foundation (project No. 20-67698.02).

References

Aalst, W. van, den Hollander, J., Peterse, W. J. A. M. & de Wolff, P. M. (1976). *Acta Cryst.* B**32**, 47–58.
Allen, F. H. (2002). *Acta Cryst.* B**58**, 380–388.
Beurskens, P. T., Beurskens, G., Bosman, W. P., de Gelder, R., Garcia-Granda, S., Gould, R. O., Israel, R. & Smits, J. M. M. (1996). *The DIRDIF*96 *Program System.* Crystallography Laboratory, University of Nijmegen, The Netherlands.
Brock, C. P. (1996). *J. Res. Natl Inst. Stand. Technol.* **101**, 321–325.
CCDC (2000). *Cambridge Structural Database*. Cambridge Crystallographic Data Centre, Cambridge, UK.
Dupont, L., Konsur, A., Lewinski, K. & Oleksyn, B. J. (1985). *Acta Cryst.* C**41**, 616–619.
Gjerløv, A. B., Kadziola, A., Petricek, V. & Larsen, S. (1995). ACA'95 Abstr. Meeting of the American Crystallographic Association.
Gjerløv, A. & Larsen, S. (1997*a*). *Acta Cryst.* B**53**, 708–718.
Gjerløv, A. B. & Larsen, S. (1997*b*). *Acta Cryst.* C**53**, 1505–1508.
Janssen, T. (1988). *Phys. Rep.* **168**, 55–113.
Janssen, T. & Janner, A. (1987). *Adv. Phys.* **36**, 519–624.

Jeffrey, G. A. (1997). *An Introduction to Hydrogen Bonding.* New York: Oxford University Press.
Kashino, S. & Haisa, M. (1983). *Acta Cryst.* C**39**, 310–312.
Larsen, S., Kozma, D. & Acs, M. (1994). *J. Chem. Soc. Perkin Trans.* 2, pp. 1091–1096.
Larsen, S. & Lopez de Diego, H. (1993). *Acta Cryst.* B**49**, 303–309.
Larsen, S., Lopez de Diego, H. & Kozma, D. (1993). *Acta Cryst.* B**49**, 310–316.
Lee, A. van der, Evain, M., Monconduit, L., Brec, R., Rouxel, J. & Petricek, V. (1994). *Acta Cryst.* B**50**, 119–128.
Lide, D. R. & Frederikse, H. P. R. (1995). *CRC Handbook of Chemistry and Physics*, 76th ed. Boca Raton: CRC Press Inc.
Marresearch (1998). Mar Image-Plate System. X-ray Research GmbH, Norderstedt, Germany.
Mettler Toledo (2000). Mettler Toledo STAR^{e} System. DSC 30 Module with TC15 TA Controller. Mettler Toledo, Greifensee, Switzerland.
Oleksyn, B. (1980). *Third Symposium on Organic Crystal Chemistry – Proceedings.* Institute of Chemistry, Adam Mickiewicz University, Poznan, Poland, pp. 232–248.
Oleksyn, B. J. (1982). *Acta Cryst.* B**38**, 1832–1834.
Oleksyn, B. J., Lebioda, L. & Ciechanowicz-Rutkowska, M. (1979). *Acta Cryst.* B**35**, 440–444.
Oleksyn, B. J. & Serda, P. (1993). *Acta Cryst.* B**49**, 530–535.
Oleksyn, B. J., Stadnicka, K. M. & Hodorowicz, S. A. (1978). *Acta Cryst.* B**34**, 811–816.
Oxford Diffraction (2001). Xcalibur Single-Crystal CCD Diffractometer. *CrysAlis Software Package.* Oxford Diffraction, Wroclaw, Poland.
Perez-Mato, J. M., Etrillard, J., Kiat, J. M., Liang, B. & Lin, C. T. (2003). *Phys. Rev. B*, **67**, 024504.
Petricek, V. & Dusek, M. (2003). *JANA*2000. Institute of Physics, Praha, Czech Republic.
Petricek, V., Gao, Y., Lee, P. & Coppens, P. (1990). *Phys. Rev. B*, **42**, 387–392.
Petricek, V., van der Lee, A. & Evain, M. (1995). *Acta Cryst.* A**51**, 529–535.
Pniewska, B. & Suszko-Purzycka, A. (1989). *Acta Cryst.* C**45**, 638–642.
Schönleber, A., Meyer, M. & Chapuis, G. (2001). *J. Appl. Cryst.* **34**, 777–779.
Sheldrick, G. M. (1997). *SHELXL*97. University of Göttingen, Germany.
Smaalen, S. van (1995). *Cryst. Rev.* **4**, 79–202.
Steed, J. W. (2003). *CrystEngCom*, **5**, 169–179.
Stoe & Cie (2002). *X-AREA*. Stoe & Cie GmbH, Darmstadt, Germany.
Suszko-Purzycka, A., Lipinska, T., Piotrowska, E. & Oleksyn, B. J. (1985). *Acta Cryst.* C**41**, 977–980.
Watkin, D. (1994). *Acta Cryst.* A**50**, 411–437.
WaveMetrics (2000). *IGOR PRO* 4.0 (*PPC*). WaveMetrics Inc., Lake Oswego, Oregon, USA.
Wolff, P. M. de (1974). *Acta Cryst.* A**30**, 777–785.
Yamamoto, A. (1996). *Acta Cryst.* A**52**, 509–560.